

Analytical Modeling of Electroosmotic and Ion Transport Flow in Nanofluidic Channels

Vishal V. R. Nandigana

Department of Mechanical Engineering, Head of Membrane Technology and Deep Learning laboratory, Fluid Systems Laboratory, Indian Institute of Technology Madras,

Chennai 600036, India, Founder of Blue Fma PVT LTD *

*Corresponding author: nandiga@iitm.ac.in, <https://bluefma.today>

Abstract: A nanofluidic channel membrane electrokinetic and ion transport analytical model, is presented for the first time. The analytical formulation is obtained by systematically solving the Poisson-Nernst-Planck and Navier-Stokes coupled multiphysics equations are simultaneously derived that matches the numerical and experimental results. The analytical formulation helps nanofluidics researchers to use the present formulation for fast simulation and validation of the experimental results.

Keywords: Analytical modeling, electroosmotic flow, ion transport, nanofluidics

1. Introduction

Nanofluidics is the study of the transport of fluids within 1-100 nm scale. Nanoporous membranes have found their use in various applications like DNA sequencing [1–3], protein sensing [4,5], fluidic circuits [6–10], desalination [11–14], and energy [15,16]. Here, the nanofluidic membrane channel allows water/ionic solution to transport through the channel under the application of typically electric field driven mediated transport [17-21]. The electric field driven transport to drive the water and ionic solution leads to the generation of current, thereby power, energy for energy production for applications, ranging from transportation, clean energy, desalination and energy source for industrial and manufacturing industries to run [15,16]. Though, large scale manufacturing of membranes at the nanoscale for various applications including energy, ionic circuits and desalination have been successfully demonstrated, the theory of nanofluidics research and science is far behind. The transport of fluids/water or ions inside nanofluidic channels needs a thorough multiscale-multiphase governing equations to solve to calculate the velocity of fluids/water and ions, and current, power for various applications being demonstrated across world today [21-28]. One of the major drawbacks of the current theories, is that though they are accurate, take tens to hundreds of thousands of hours of computational time to solve and requires thousands of processors for the equations to run in the server [21-28]. The large computational time limits researchers to calculate a large number of designs to best design the nanofluidic membrane channels for myriad applications at present and also new applications in the future.

In this paper, we consider the accurate theory of Poisson-Nernst-Planck equation coupled with Navier-Stokes equations, and derive analytical derivations, for this multiscale multiphase multiphysics interactions involved nanofluidic channel transport, accounting for the solid-liquid interactions between the nanofluidic channel wall and the fluid/water and ionic electrolyte species interactions, accounting for the surface governed transport contributions and extreme nanoscale confinement effects.

2. Mathematical Modelling

The PNP+NS equations are analytically derived, accurately with no loss of terms or order of PDEs in the final analytical solution. The classical PNP equation is given by,

$$\nabla \cdot (\epsilon_r \nabla \phi) = \frac{-\rho_e}{\epsilon_0} \quad (1)$$

$$\frac{\partial c_i}{\partial t} = -\nabla \cdot \mathfrak{J}_i \quad (2)$$

$$\mathfrak{J}_i = -D_i \nabla c_i - \frac{D_i z_i F c_i}{RT} \nabla \phi + c_i u \quad (3)$$

The Nernst-Planck equation without electro neutrality

$$\frac{\partial c_i}{\partial t} = -\nabla \cdot \left(-D_i \nabla c_i - \frac{D_i z_i F c_i}{RT} \nabla \phi + c_i u \right) \quad (4)$$

Steady state Nernst-Planck equation (under equilibrium zero voltage input and electrokinetic velocity, $u = 0$)

$$\mathfrak{J} = -D \left(\nabla c + \frac{zF}{RT} c (\nabla \phi) \right) \quad (5)$$

To calculate the nonequilibrium, under applied voltage, electrokinetic fluid/water transport, we solve, Navier-Stokes equation, given below.

$$\rho \left(\frac{\partial u}{\partial t} + u \cdot \nabla u \right) = -\nabla P + \mu \nabla^2 u - \sum_{i=1}^m z_i F c_i \nabla \phi \quad (6)$$

$$\rho_e = F \sum_{x=1}^m z_i c_i \quad (7)$$

$$E = -\nabla \phi$$

$$\rho \left(\frac{\partial u}{\partial t} + u \cdot \nabla u \right) = -\nabla P + \mu \nabla^2 u + \rho_e E \quad (8)$$

ϕ , is the electrostatic potential

\mathfrak{J}_i is the flux vector of each ionic species, i

c_i is concentration ion species, i

m , number of ionic electrolyte species

P , is pressure

ρ_e is net space charge density

ϵ_0 is permittivity of free space (vacuum permittivity)

ϵ_r is relative permittivity of medium

z_i is valence of ion species

D_i is diffusion coefficient of ion species

μ is dynamic viscosity

μ_i is mobility of ion species

ρ is fluid/water density

u , is fluid/water velocity

E , is electric field

F , is Faraday constant

R , is gas constant

T , is Temperature

t, is time.

3. Analytical Derivation

A) Local space charge density distribution along the axial direction

$$\rho_e(x) = Ae^{\frac{\sqrt{\beta}}{\lambda_D}x} + e^{-\frac{\sqrt{\beta}}{\lambda_D}x} - \frac{2\sigma}{h} \quad (9)$$

where σ is the surface charge density of the nanofluidic channel membrane, of length, L and height, h.

Boundary conditions

$$\begin{aligned} \rho_e(x) &= 0 \text{ at } x = 0 \\ \rho_e(x) &= 0 \text{ at } x = L \end{aligned}$$

Substituting boundary conditions to Eq. (9), we obtain

$$\rho_e(x) = \frac{2\sigma}{h(1+\alpha_x)} \left[e^{\frac{\sqrt{\beta}}{\lambda_D}x} + \alpha_x e^{-\frac{\sqrt{\beta}}{\lambda_D}x} \right] \quad (10)$$

$$\lambda_D = \sqrt{\frac{\epsilon_0 \epsilon_r RT}{2z^2 F^2 C_b}} \quad (11)$$

λ_D is the Debye length, z is the valence of the bigger electrolyte ionic species, respectively, C_b is the bulk ionic electrolyte solution concentration.

$$\begin{aligned} \alpha_x &= e^{\frac{\sqrt{\beta}L}{\lambda_D}} \\ \beta &= \sqrt{\frac{C_n^2}{4C_b^2} + 1} \end{aligned}$$

where C_n is nanochannel fixed charge concentration, that can be held by the nanofluidic channel design and geometry and surface charge density, σ .

B) The electric potential distribution along the axial direction

From the poisson equation (2-D)

$$\frac{\partial^2 \varphi}{\partial x^2} + \frac{\partial^2 \varphi}{\partial y^2} = \frac{-\rho_e}{\epsilon_0 \epsilon_r} \quad (12)$$

Integrating over the surface of the nanofluidic channel, taking into effect the channel surface boundary conditions, given as,

$$\frac{\partial \varphi}{\partial y} = \frac{-\sigma}{\epsilon_0 \epsilon_r} \quad \text{at } y = 0$$

$$\frac{\partial \varphi}{\partial y} = \frac{\sigma}{\epsilon_0 \epsilon_r} \quad \text{at } y = h, \text{ nanochannel height}$$

The electric potential distribution along the axial direction is given as,

$$\varphi(x) = \frac{-2\sigma}{h\epsilon_0 \epsilon_r} \left(\frac{1}{1+\alpha_x} \right) \frac{\lambda_D^2}{\beta} e^{\frac{\sqrt{\beta}}{\lambda_D}x} - \frac{2\sigma}{h\epsilon_0 \epsilon_r} \left(\frac{\alpha_x}{1+\alpha_x} \right) \frac{\lambda_D^2}{\beta} e^{-\frac{\sqrt{\beta}}{\lambda_D}x} + J_1 x + J_2 \quad (13)$$

The axial potential boundary conditions are given as,

$$\begin{aligned} \varphi(x) &= \varphi_L \text{ at } x = 0 \\ \varphi(x) &= \varphi_R \text{ at } x = L \end{aligned} \quad (14)$$

where φ_L is the potential applied at the source end and φ_R is the potential applied at the drain end of the nanofluidic channel system.

Solving, Eq. (13) with boundary conditions, specified in Eq. (14), the electric potential distribution along the axial direction is given as,

$$\begin{aligned} \varphi(x) &= \frac{-2\sigma}{h\epsilon_0 \epsilon_r} \left(\frac{1}{1+\alpha_x} \right) \frac{\lambda_D^2}{\beta} \left(e^{\frac{\sqrt{\beta}}{\lambda_D}x} + \alpha_x e^{-\frac{\sqrt{\beta}}{\lambda_D}x} \right) + \left(\frac{\varphi_R - \varphi_L}{L} \right) x + \\ &\varphi_L + \frac{2\sigma}{h\epsilon_0 \epsilon_r} \frac{\lambda_D^2}{\beta} \end{aligned} \quad (15)$$

C) Concentration of two-ionic electrolyte species distribution along the axial direction

C1) anion concentration along the axial direction

$$c_1(x) = K_1 e^{-\frac{zF}{RT}\varphi(x)} + e^{-\frac{zF}{RT}\varphi(x)} \int_0^x P e^{-\frac{zF}{RT}\varphi(\zeta)} d\zeta + R \quad (16)$$

Boundary conditions

$$c_1(x) = C_b \text{ at } x = 0$$

$$c_1(x) = C_b \text{ at } x = L$$

$$K_1 =$$

$$\frac{\left(\frac{C_n + C_b \beta - C_b \right) L}{2}}{\int_0^L \left[\frac{e^{-\frac{zF}{RT}\varphi(x)}}{e^{-\frac{zF}{RT}\varphi R}} \left(\frac{e^{-\frac{zF}{RT}\varphi(x)}}{e^{-\frac{zF}{RT}\varphi L}} \right) \int_0^x \frac{e^{-\frac{zF}{RT}\varphi(\zeta)}}{e^{-\frac{zF}{RT}\varphi L}} d\zeta - \frac{e^{-\frac{zF}{RT}\varphi L}}{\int_0^L \frac{e^{-\frac{zF}{RT}\varphi(\zeta)}}{e^{-\frac{zF}{RT}\varphi L}} d\zeta} \right] dx} \quad (17)$$

$$P = \frac{-K_1 \left[\frac{e^{-\frac{zF}{RT}\varphi R}}{e^{-\frac{zF}{RT}\varphi L}} - \frac{e^{-\frac{zF}{RT}\varphi L}}{e^{-\frac{zF}{RT}\varphi R}} \right]}{e^{-\frac{zF}{RT}\varphi R} \int_0^L \frac{e^{-\frac{zF}{RT}\varphi(\zeta)}}{e^{-\frac{zF}{RT}\varphi L}} d\zeta} \quad (18)$$

$$R = C_b - K_1 e^{-\frac{zF}{RT}\varphi L} \quad (19)$$

C2) Cation concentration along the axial direction

Using, space charge density Eq. (7), we calculate the cation concentration,

$$c_2(x) = \frac{\rho_e - z_1 F c_1}{z_2 F} \quad (20)$$

Using Eq. (20) and Nernst-Planck equation, Eq. (4), the cation concentration, $c_2(x)$ is given as,

$$c_2(x) = K_2 e^{\frac{zF}{RT}\varphi(x)} + e^{\frac{zF}{RT}\varphi(x)} \int_0^x Q e^{-\frac{zF}{RT}\varphi(\zeta)} d\zeta + S \quad (21)$$

with the boundary conditions,

$$c_2(x) = C_b \quad \text{at } x = 0$$

$$c_2(x) = C_b \quad \text{at } x = L$$

$$K_2 = \frac{\left(-\frac{C_n}{2} + C_b \beta - C_b \right) L}{\int_0^L \left[\frac{e^{\frac{zF}{RT}\varphi(x)}}{e^{\frac{zF}{RT}\varphi R}} \left(\frac{e^{\frac{zF}{RT}\varphi(x)}}{e^{\frac{zF}{RT}\varphi L}} \right) \int_0^x \frac{e^{-\frac{zF}{RT}\varphi(\zeta)}}{e^{-\frac{zF}{RT}\varphi L}} d\zeta - \frac{e^{\frac{zF}{RT}\varphi L}}{\int_0^L \frac{e^{-\frac{zF}{RT}\varphi(\zeta)}}{e^{-\frac{zF}{RT}\varphi L}} d\zeta} \right] dx} \quad (22)$$

$$Q = \frac{-K_2 \left[\frac{e^{\frac{zF}{RT}\varphi R}}{e^{\frac{zF}{RT}\varphi L}} - \frac{e^{\frac{zF}{RT}\varphi L}}{e^{\frac{zF}{RT}\varphi R}} \right]}{e^{\frac{zF}{RT}\varphi R} \int_0^L \frac{e^{-\frac{zF}{RT}\varphi(\zeta)}}{e^{-\frac{zF}{RT}\varphi L}} d\zeta} \quad (23)$$

$$S = C_b - K_2 \left[e^{\frac{zF}{RT}\varphi L} \right] \quad (24)$$

D) Space charge density distribution, ρ_e , across the nanofluidic channel height

From, Eq. (2) and Eq. (7), we obtain,

$$\rho_e(y) = P_1 e^{\frac{\sqrt{\beta}}{\lambda_D}y} + P_2 e^{-\frac{\sqrt{\beta}}{\lambda_D}y} \quad (25)$$

with boundary conditions obtained from Eq. (1), Eq. (2) and Eq. (7),

$$\frac{\partial \rho_e(y)}{\partial y} = \frac{\beta \sigma}{\lambda_D} \text{ at } y = 0$$

$$\frac{\partial \rho_e(y)}{\partial y} = \frac{-\beta \sigma}{\lambda_D} \text{ at } y = h, \text{ nanochannel height}$$

we arrive,

$$\rho_e(y) = \frac{-1}{\alpha_y - 1} \frac{\sqrt{\beta}}{\lambda_D} \sigma \left[e^{\frac{\sqrt{\beta}}{\lambda_D} y} + \alpha_y e^{-\frac{\sqrt{\beta}}{\lambda_D} y} \right] \quad (26)$$

$$\alpha_y = e^{\frac{\sqrt{\beta}}{\lambda_D} h}$$

E) Electric potential distribution across the nanofluidic channel height

From Eq. (1) and Eq. (7), we obtain,

$$\varphi(y) = \frac{\sigma}{\alpha_y - 1} \frac{\lambda_D}{\sqrt{\beta} \epsilon_0 \epsilon_r} \left[e^{\frac{\sqrt{\beta}}{\lambda_D} y} + \alpha_y e^{-\frac{\sqrt{\beta}}{\lambda_D} y} \right] + P_3 y + P_4 \quad (27)$$

with boundary conditions

$$\frac{\partial \varphi(y)}{\partial y} = \frac{-\sigma}{\epsilon_0 \epsilon_r} \quad \text{at } y = 0$$

$$\frac{\partial \varphi(y)}{\partial y} = \frac{\sigma}{\epsilon_0 \epsilon_r} \quad \text{at } y = h$$

On solving Eq. (27) with the above boundary conditions, we obtain,

$$\varphi(y) = \frac{\sigma}{\alpha_y - 1} \frac{\lambda_D}{\sqrt{\beta} \epsilon_0 \epsilon_r} \left[e^{\frac{\sqrt{\beta}}{\lambda_D} y} + \alpha_y e^{-\frac{\sqrt{\beta}}{\lambda_D} y} \right] + \varphi(x) - \frac{2\sigma \lambda_D^2}{\beta \epsilon_0 \epsilon_r h} \quad (28)$$

F) Concentration of two-ionic electrolyte species distribution across the nanofluidic channel height

F1) anion concentration across the nanofluidic channel height

From, Eq. (4), we obtain the anion concentration across the nanofluidic channel height, given as,

$$c_1(y) = \frac{c_1(x)}{\frac{1}{h} \int_0^h e^{\frac{-zF}{RT} \varphi(y)} dy} e^{\frac{-zF}{RT} \varphi(y)} \quad (29)$$

F2) cation concentration across the nanofluidic channel height

From, Eq. (4), we obtain the cation concentration across the nanofluidic channel height, given as,

$$c_2(y) = \frac{c_2(x)}{\frac{1}{h} \int_0^h e^{\frac{-zF}{RT} \varphi(y)} dy} e^{\frac{zF}{RT} \varphi(y)} \quad (30)$$

G) Solving for the contour water/fluid electrokinetic 2D motion inside the nanofluidic channel

Solving Eq. (8), assuming fluid/water flow is uniform and well developed along the axial direction and the water/fluid electrokinetic transport varies across the nanofluidic channel height, the 2D water/fluid electrokinetic transport velocity profile, is given by,

$$u = \int \int \left[\frac{1}{\mu} \left(\frac{\partial P}{\partial x} + \rho_e(x) \frac{\partial \varphi(x)}{\partial x} \right) dy \right] dy + P_5 y + P_6 \quad (31)$$

where the water/fluid boundary conditions are given as,

$$(u)_{y=0} = 0 \quad \text{No slip condition}$$

$$(u)_{y=h} = 0 \quad \text{No slip condition}$$

Solving Eq. (31) with the above boundary conditions, give us,

$$P_5 = 0$$

$$P_6 = \frac{\sigma}{\mu(\alpha_y - 1)} \left(\frac{\lambda_D}{\sqrt{\beta}} \right) (1 + \alpha_y) \left[\frac{1}{\alpha_x + 1} \left(\frac{-2\sigma}{h \epsilon_0 \epsilon_r} \right) \frac{\lambda_D}{\sqrt{\beta}} \left(e^{\frac{\sqrt{\beta}}{\lambda_D} x} - axe^{-\beta \lambda_D x} + \varphi R - \varphi LL + P6 \right) \right] \quad (32)$$

u =

$$\frac{1}{\mu} \frac{-\sigma}{(\alpha_y - 1)} \left(\frac{\lambda_D}{\sqrt{\beta}} \right) \left(e^{\frac{\sqrt{\beta}}{\lambda_D} y} + \alpha_y e^{-\frac{\sqrt{\beta}}{\lambda_D} y} \right) \left[\frac{1}{\alpha_x + 1} \left(\frac{-2\sigma}{h \epsilon_0 \epsilon_r} \right) \frac{\lambda_D}{\sqrt{\beta}} \left(e^{\frac{\sqrt{\beta}}{\lambda_D} x} - axe^{-\beta \lambda_D x} + \varphi R - \varphi LL + P6 \right) \right] \quad (33)$$

Numerical Simulations

The analytical derivation for water/fluid electrokinetic transport and ionic electrolyte species transport inside nanofluidic channel systems are compared with our in-house developed numerical simulations. We use OpenFOAM platform based open source, freely accessible, open source package platform and in-house developed PNP+NS numerical simulation solvers [21-28] to compare our analytical derivation solutions. The PNP+NS numerical software platform package is available in the GitHub, under free access and download at https://github.com/nandiga/PNP_Navier_Stokes_Foam

Nanofluidic channel geometry

Here, nanofluidic channel geometry of length 500 nm and 30 nm height is considered. The steady state zero voltage equilibrium electrokinetic water/fluid transport and ion transport is compared between numerical simulations and analytical derivations. The inlet supplied concentration, for a KCl electrolyte solution is 0.1 mM, and the nanofluidic channel surface charge density here is $\sigma = -1 \text{ mC/m}^2$. Further, the analytical derivation solution is compared with the experiments of Cheng et al.[29]. 3D homogenous Silica nanochannels[29] of two geometries, dimensions, Length, L = 60 μm, width w = 2.5 μm X 5 and height h = 18.7 nm and geometry (2) has dimensions, Length, L = 60 μm, width w = 2.5 μm X 5 and height h = 4 nm, respectively. KCl concentration is varying across 5 orders of magnitude from 10⁻⁵ M to 1 M.

4. Results

Fig. 1. shows the steady state zero voltage equilibrium electrokinetic water/fluid transport and ionic electrolyte species transport between numerical simulations and analytical derivation solutions. The 2D numerical PNP+NS simulations and the analytical derivations results match to 99% accuracy. Fig. 2. shows the conductance (S) results comparison between Cheng et al.[29] experiments and the analytical derivation solutions. The results match exceedingly well (almost 100% match) between Cheng et al. [29] experimental results and the analytical derivation solutions. The nanofluidic channel surface charge density was kept as a free parameter and varied to match Cheng et al. [29] experimental results as the surface charge density of the nanofluidic channel was not known in their experimental studies.

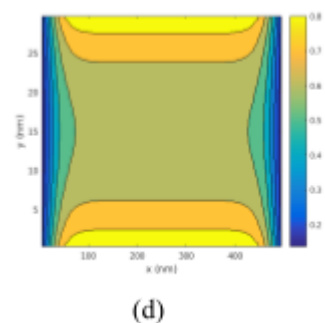
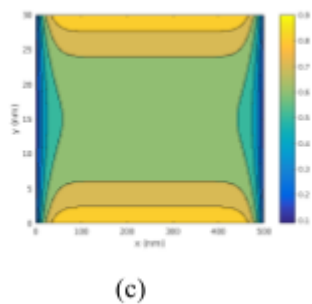
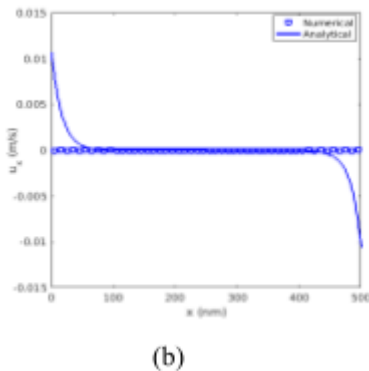
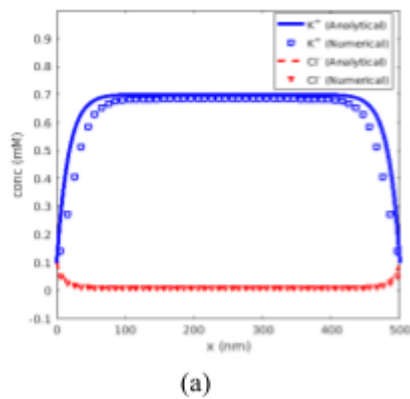


Figure 1: (a) Comparison between numerical simulation with analytical derivation for axial ion transport of KCl electrolyte concentration distribution inside nanofluidic channel, with nanofluidic channel wall surface charge density, $\sigma = -1 \text{ mC/m}^2$. (b) Comparison between numerical simulation with analytical derivation for axial water/fluid electrokinetic transport, under zero voltage, equilibrium transport. (c-d) Comparison between analytical derivation (Fig. 1c) and numerical simulation (Fig. 1d) for contour 2D ionic electrolyte transport, KCl, inside 2D nanofluidic geometry channel. The analytical derivation matches close to 99% accuracy to the numerical simulation.

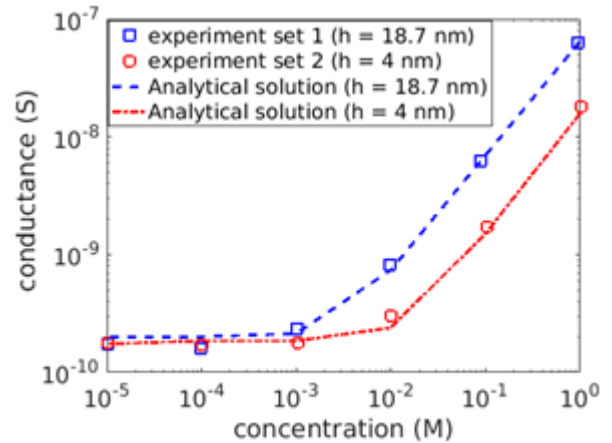


Figure 2: Comparison between Cheng et. al.[29] experimental conductance for two different geometries of homogenous silica nanofluidic channel with our analytical derivation solution conductance.

5. Conclusions

Here, we present an analytical derivation solution for a nanofluidic channel system to calculate the electrokinetic water/fluid transport and ion electrolyte species transport, along with conductance results for the first time. The analytical formulation matches very well (close to 99% accuracy) with the complete 2D PNP+NS numerical simulations and published experimental literature results for nanofluidic channel systems.

References

- [1] Z. Yuan, Y. Liu, M. Dai, X. Yi, and C. Wang, *Controlling DNA Translocation Through Solid-State Nanopores*, *Nanoscale Res. Lett.* 15, 80 (2020).
- [2] Y. Zhang, Y. Zhou, Z. Li, H. Chen, L. Zhang, and J. Fan, *Computational Investigation of Geometrical Effects in 2D Boron Nitride Nanopores for DNA Detection*, *Nanoscale* 12, 10026 (2020).
- [3] G. F. Schneider and C. Dekker, *DNA Sequencing with Nanopores*, *Nat. Biotechnol.* 30, 326 (2012).
- [4] D. W. Deamer and D. Branton, *Characterization of Nucleic Acids by Nanopore Analysis*, *Acc. Chem. Res.* 35, 817 (2002).
- [5] S. Cabello-Aguilar, S. Balme, A. A. Chaaya, M. Bechelany, E. Balanzat, J.-M. Janot, C. Pochat-Bohatier, P. Miele, and P. Dejardin, *Slow Translocation of Polynucleotides and Their Discrimination by α -Hemolysin inside a Single Track-Etched Nanopore Designed by Atomic Layer Deposition*, *Nanoscale* 5, 9582 (2013).
- [6] S. H. Han, S.-R. Kwon, S. Baek, and T.-D. Chung, *Ionic Circuits Powered by Reverse Electrodialysis for an Ultimate Iontronic System*, *Sci. Rep.* 7, 14068 (2017).
- [7] M. Ali, S. Mafe, P. Ramirez, R. Neumann, and W. Ensinger, *Logic Gates Using Nanofluidic Diodes Based on Conical Nanopores Functionalized with Polyprotic Acid Chains*, *Langmuir* 25, 11993 (2009).
- [8] J.-H. Han, K. B. Kim, H. C. Kim, and T. D. Chung, *Ionic Circuits Based on Polyelectrolyte Diodes on a Microchip*, *Angew. Chemie Int. Ed.* 48, 3830 (2009).

- [9] R. A. Lucas, C.-Y. Lin, L. A. Baker, and Z. S. Siwy, *Ionic Amplifying Circuits Inspired by Electronics and Biology*, Nat. Commun. 11, 1568 (2020).
- [10] T. S. Plett, W. Cai, M. Le Thai, I. V Vlassiouk, R. M. Penner, and Z. S. Siwy, *Solid-State Ionic Diodes Demonstrated in Conical Nanopores*, J. Phys. Chem. C 121, 6170 (2017).
- [11] M. Heiranian, A. B. Farimani, and N. R. Aluru, *Water Desalination with a Single-Layer MoS₂ Nanopore*, Nat. Commun. 6, 8616 (2015).
- [12] V. P. K., S. K. Kannam, R. Hartkamp, and S. P. Sathian, *Water Desalination Using Graphene Nanopores: Influence of the Water Models Used in Simulations*, Phys. Chem. Chem. Phys. 20, 16005 (2018).
- [13] B. Corry, *Water and Ion Transport through Functionalised Carbon Nanotubes: Implications for Desalination Technology*, Energy Environ. Sci. 4, 751 (2011).
- [14] J. Palmeri, N. Ben Amar, H. Saidani, and A. Deratani, *Process Modeling of Brackish and Seawater Nanofiltration*, Desalin. Water Treat. 9, 263 (2009).
- [15] M. Macha, S. Marion, V. V. R. Nandigana, and A. Radenovic, *2D Materials as an Emerging Platform for Nanopore-Based Power Generation*, Nat. Rev. Mater. 4, 588 (2019).
- [16] J. Feng, M. Graf, K. Liu, D. Ovchinnikov, D. Dumcenco, M. Heiranian, V. Nandigana, N. R. Aluru, A. Kis, and A. Radenovic, *Single-Layer MoS₂ Nanopores as Nanopower Generators*, Nature 536, 197 (2016).
- [17] R. M. M. Smeets, U. F. Keyser, D. Krapf, M.-Y. Wu, N. H. Dekker, and C. Dekker, *Salt Dependence of Ion Transport and DNA Translocation through Solid-State Nanopores*, Nano Lett. 6, 89 (2006).
- [18] S. Balme, F. Picaud, M. Manghi, J. Palmeri, M. Bechelany, S. Cabello-Aguilar, A. Abou-Chaaya, P. Miele, E. Balanzat, and J. M. Janot, *Ionic Transport through Sub-10 Nm Diameter Hydrophobic High-Aspect Ratio Nanopores: Experiment, Theory and Simulation*, Sci. Rep. 5, 10135 (2015).
- [19] C. Ho, R. Qiao, J. B. Heng, A. Chatterjee, R. J. Timp, N. R. Aluru, and G. Timp, *Electrolytic Transport through a Synthetic Nanometer-Diameter Pore*, Proc. Natl. Acad. Sci. U. S. A. 102, 10445 LP (2005).
- [20] W. C. Swope, H. C. Andersen, P. H. Berens, and K. R. Wilson, *A Computer Simulation Method for the Calculation of Equilibrium Constants for the Formation of Physical Clusters of Molecules: Application to Small Water Clusters*, J. Chem. Phys. 76, 637 (1982).
- [21] V. V. R. Nandigana, M. Heiranian and N. R. Aluru, *Single ion transport with a single-layer graphene nanopore*, International Journal of Mechanical and Mechatronics Engineering, 13, 2019.
- [22] V. V. R. Nandigana, K. D. Jo, A. T. Timperman and N. R. Aluru, *Asymmetric-Fluidic-Reservoirs Induced High Rectification Nanofluidic diode*, Sci. Rep., 8, 1-10, 2018.
- [23] V. V. R. Nandigana and N. R. Aluru, *1/f pink chaos in nanopores*, RSC Advances, 7, 46092-46100, 2017.
- [24] V. V. R. Nandigana and N. R. Aluru, *Avalanche effects near nano-junctions*, Phys. Rev. E, 94, 012402, 2016.
- [25] H. Wang, V. V. R. Nandigana, K. Jo, N. R. Aluru and A. Timperman, *Controlling the Ionic Current Rectification Factor of a Nanofluidic-Microfluidic Interface with Symmetric Nanocapillary Interconnects*, Anal. Chem., 87, 3598-3605, 2015.
- [26] V. V. R. Nandigana and N. R. Aluru, *Characterization of electrochemical properties of a micro-nanochannel integrated system using computational impedance spectroscopy CIS*, Electrochimica Acta, 105, 514-523, 2013.
- [27] V. V. R. Nandigana and N. R. Aluru, *Nonlinear Electrokinetic Transport Under Combined ac and dc Fields in Micro-Nanofluidic Interface Devices*, Journal of Fluids Engineering, 135, 021201, 2013.
- [28] V. V. R. Nandigana and N. R. Aluru, *Understanding anomalous current-voltage characteristics in microchannel-nanochannel interconnect devices*, JCIS, 384, 162-171, 2012.
- [29] Li-Jing Cheng and L. J. Guo, *Rectified Ion Transport through Concentration Gradient in Homogeneous Silica Nanochannels*, Nano Lett. 2007, 7, 10, 3165-3171